ACS Partner Journal

ACCOUNTS
—of materials research—

pubs.acs.org/amrcda

Article

New Applications of Zirconium Phosphate Nanomaterials

Mario V. Ramos-Garcés,[#] Julissa González-Villegas,[#] Aleannette López-Cubero,[#] and Jorge L. Colón*

Cite This: *Acc. Mater. Res.* 2021, 2, 793−803

Read Online

ACCESS | Metrics & More | Article Recommendations | Supporting Information

CONSPECTUS: The 2-D layers of the inorganic ion exchanger α-zirconium phosphate ($Zr(HPO_4)_2{\cdot}H_2O$, α-ZrP) make this compound particularly stable to low pH, high temperature, and ionizing radiation. Initially studied for its ion exchange properties, once the conditions for its synthesis in crystalline form was accomplished by James Stynes and Abraham Clearfield in 1964, numerous other types of studies and applications followed. Extensive studies in the 1960s and 1970s on the thermodynamics of ion exchange led to insights into the intercalation mechanism of this material. The Clearfield group solved the crystal structure in 1968 and refined it in 1977. Powder methods were pioneered by the Clearfield group to solve the structure of this type of materials. In 1968 Giulio Alberti reported means to prepare zirconium phosphonates expanding the chemistry of these layered compounds. New phases of ZrP were also discovered (e.g., γ, θ, λ, τ) and the applications ranged from heterogeneous catalysis to intercalation chemistry and solid-state proton conductors. Methods to exfoliate the layers of ZrP were developed in the 1990s as interest grew in new applications of these types of materials. For example, protein and enzyme intercalation was accomplished starting in the 1990s by the McLendon, Mallouk, and Kumar groups. In the early 2000s, the Colón group pioneered the use of the θ phase of ZrP for the direct intercalation of large inorganic metal complexes that could not be directly intercalated into the α phase. Initial studies in the Colón group ranged from applications of these directly intercalated ZrP derivatives in photophysics and photochemistry, amperometric biosensors, vapochromism, and vapoluminescence. Over the past decade, new applications of these materials have been developed in anticancer drug delivery and electrocatalysis of the oxygen evolution reaction (OER). ZrP has now proven to be a promising drug nanocarrier and its unique chemical microenvironment provided by the α-type layers and the interlayer space enhances catalytic activity for numerous types of reactions. Further elucidation of the catalytic active species under operando conditions as well as the chemical structure of drug-intercalated derivatives should provide new insights that will advance the design and development of new compounds with desired properties. The initial pioneering efforts of Clearfield and Alberti are being continued by numerous research groups providing new exciting areas of development on the chemistry of layered M(IV) phosphate and phosphonate compounds. In this Account we present the efforts of the Colón group during the past decade on studies of the applications of ZrP for anticancer drug delivery and electrocatalysis of the OER.

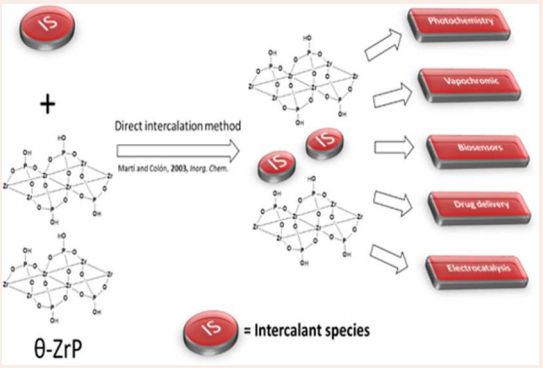

INTRODUCTION

The inorganic layered material zirconium phosphate ($Zr(HPO_4)_2{\cdot}H_2O$, α-ZrP) has a long and illustrious history.[1−4] After initial work on the synthesis of amorphous ZrP, strong interest in this material surged in the 1950s as its ion-exchange properties were found to be excellent for wastewater remediation in the nuclear industry.[5] In 1964, Stynes and Clearfield reported for the first time the synthesis of crystalline ZrP using reflux methods with high concentrations of H_3PO_4,[6] which opened new opportunities to explore the characteristics and properties of this material. By 1968, the X-ray crystal structure of α-ZrP was determined by Smith and Clearfield[7] and refined by Troup and Clearfield in 1977.[8] Its structure (Figure 1) consists of zirconium atoms aligned in an almost perfect plane, with phosphate groups on both sides of the plane joining the Zr ions in bridges, forming octahedra having Zr atoms at their center with the six corners being oxygens of the adjacent phosphate groups and tetrahedra of phosphate groups on top and the below of each of the ZrP atoms' planes, with P atoms at the center of the tetrahedra formed by oxygens. The interlayer distance for the α phase is 7.6 Å. The fourth oxygen of the phosphate groups points almost perpendicularly to the Zr atoms' plane and carries an acidic hydrogen. Proton exchange is the premier intercalation process and the reason why ZrP has been used in separation studies and acidic catalysis.[9−12]

The Clearfield group pioneered the study of the thermodynamics and kinetics of the ion-exchange reactions of ZrP and

Received: May 3, 2021
Revised: June 28, 2021
Published: September 1, 2021

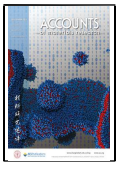

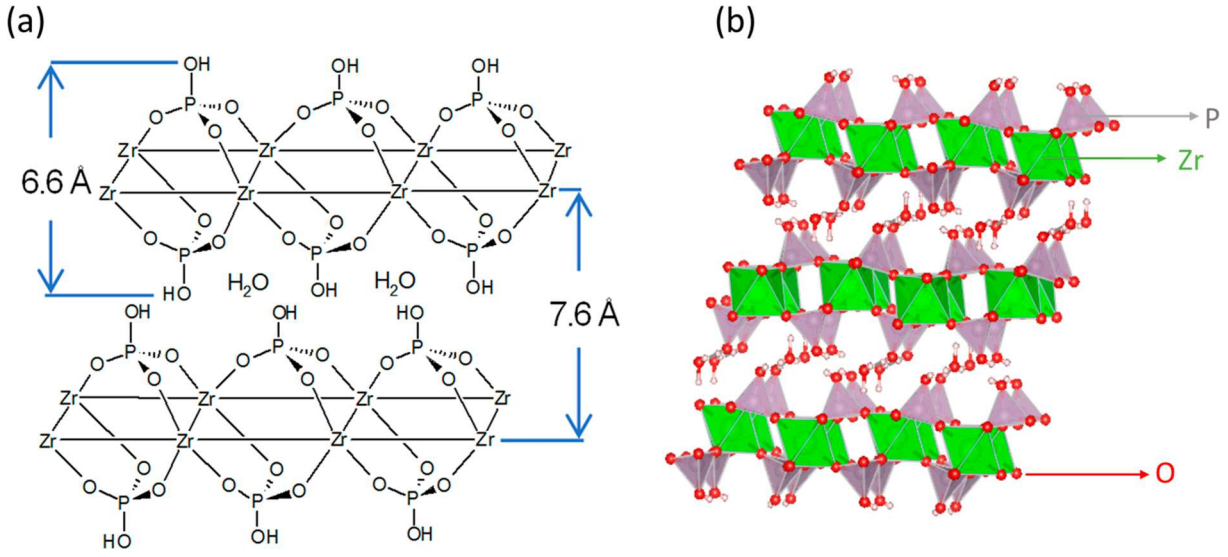

Figure 1. (a) The structure of α-ZrP. (b) Polyhedral model of the structure of α-ZrP. Reproduced with permission from ref 53. Copyright 2020 IntechOpen.

Scheme 1. ZrP as Drug Nanocarriers of Intercalated Species (IS)

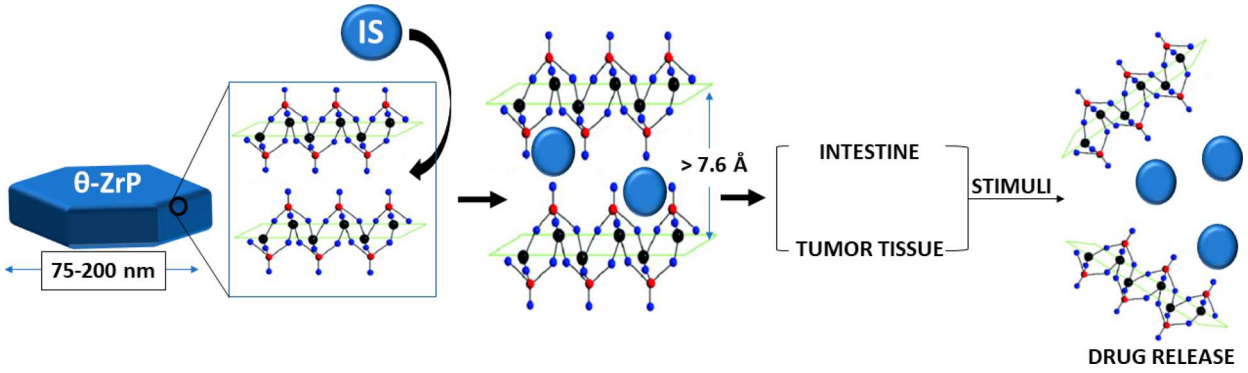

started to explore its catalytic activity. In addition, in 1968, Alberti's group at the University of Perugia pioneered a simpler method to obtain crystalline ZrP based on first preparing a fluoride complex that slowly released Zr^{4+} ions to a H_3PO_4 solvent and rapidly precipitated the crystalline ZrP phase.[13] This group also advanced the study of a second phase of ZrP, the γ phase, which, with two types of phosphate groups instead of only one, has a larger interlayer distance of 11.2 Å. In addition, the Alberti group developed methods to prepare zirconium phosphonates in 1978;[14] a large variety of single and mixed zirconium phosphates and phosphonates were developed by the Alberti and the Clearfield groups in both sides of the Atlantic.

For the next 50 years, new developments included the study of the ion-exchange and intercalation chemistry of these materials,[10−12,15] new nanophases and hybrid materials,[16] layer exfoliation,[17] surface modification,[18] and the application of these materials in catalysis, fuel cells,[19] photophysics and photochemistry,[20] electron-transfer reactions and amperometric biosensors,[21−23] vapochromic materials,[24] protein adsorption and intercalation,[17,25] and lubricant additives.[26]

The untimely death of Alberti and the recent retirement of Clearfield closes an epoch in zirconium phosphate studies. Both left as legacy numerous students, postdoctoral research associates, and collaborators that have continued their interest into new applications of these materials.

Our independent foray into this field occurred in the early 2000s, when we were able to directly intercalate tris(2,2′-bipyridine)ruthenium(II) ($[Ru(bpy)_3]^{2+}$) into a highly hydrated phase of ZrP, $Zr(HPO_4)_2{\cdot}6H_2O$ (θ-ZrP), whose facile synthesis had been developed by Kijima in 1982.[27] The θ-ZrP phase has α-type layers but has six water molecules per formula unit instead of one, and as a consequence, its interlayer distance is 10.4 Å. The expanded interlayer distance permits the intercalation of luminescent metal complexes, as first shown by Martí and Colón in 2003.[21] The direct intercalation of $[Ru(bpy)_3]^{2+}$ was followed by intercalation studies of Re, Co, Fe, and Pt compounds, for possible applications in photochemistry, amperometric biosensors, and vapochromism.[22−24,28] More recently, our group has been involved in studying new applications of ZrP for anticancer drug delivery and electrocatalysis for the oxygen evolution reaction (OER).

In this Account we summarize those new developments made by our group in the past decade.

ZIRCONIUM PHOSPHATE AS A PROMISING DRUG NANOVEHICLE

Designing a drug delivery system with high organ or tissue specificity is one of the biggest challenges in cancer nanotherapy. The use of nanoparticles as drug carriers has been proposed to induce selective targeting and to reduce drug's toxicity and

https://doi.org/10.1021/accountsmr.1c00102
Acc. Mater. Res. 2021, 2, 793−803

resistance.[29−31] A good nanocarrier must fulfill several criteria such as high drug loading capacity, be able to trigger the cargo, stealth, serum and plasma stability, nonimmunogenicity, good cellular uptake, and be able to be cleared to avoid accumulation. Different nanoparticles, such as liposomes,[32] polymeric micelles,[33] and lipids,[34] among others, have been developed as spherical drug nanocarriers. However, many of these nanoparticles have demonstrated poor oral bioavailability, instability under serum conditions or toxicity, which compromises the patient's clinical safety.[35,36]

During the past decade, our group has investigated ZrP as a platform for drug delivery applications (Scheme 1). Some of the properties that make ZrP very attractive as a drug nanocarrier are versatility, robustness, thermal and chemical stability, high ion exchange capacity of 6.64 mequiv·g^{-1} to incorporate high concentration of drugs (the loaded drugs' cations exchange with the protons of phosphate groups), stability under physiological conditions, resolved crystal structure, nontoxicity, and not being related to metabolic functions.[37] In addition, the drug release can be triggered by pH stimuli, possesses a modifiable surface,[37] and the nanoparticles have a size of 70−200 nm and a platelet shape.[38] Furthermore, its size should allow it to accumulate in tumor tissue due to the enhanced permeability and retention (EPR) effect: the increased permeability of nanoparticles from blood vessels to the tumor tissue occurring through fenestrations (gaps) on the cell surface (diameter size: up to 800 nm) formed as a result of a poor cellular packing of the tumoral blood vessels tissue and the accumulation or retention of nanoparticles in the tumor tissue caused by a deficient lymphatic system (see Figure S1).[30,39] Therefore, ZrP nanoparticle size is adequate to pass through fenestrations and consequently being selectively accumulated in the tumor tissue. Additionally, the platelet-like shape of ZrP makes it very attractive as a nanocarrier since it promotes an enhanced extravasation contrary to spherical nanoparticles, which tend to stay in the center of the capillary blood flow disrupting this process.[40,41]

ZrP Biocompatibility

The biocompatibility of ZrP materials was studied by our group and our collaborators. Cell viability assays demonstrated that ZrP nanoplatelets by themselves do not induce cytotoxic effects in several normal and cancer cell lines such as human kidney, macrophages, breast, and ovarian cancer cells.[42,43] Furthermore, we suggest that the size and shape of ZrP results in improvements in the margination, adherence to endothelial walls, and cellular internalization by endocytosis.[31,39] ZrP nanoplatelet shape has higher propensity to tumbling in blood vessels, which promotes the contact between the nanoplatelet and the endothelial tissue and extravasation,[40] enhancing the EPR effect, one of the bases for anticancer drug delivery nanotechnology.[41]

Our group has exploited the use of the highly hydrated θ-ZrP phase to intercalate different therapeutic agents; its expanded interlayer distance allows the direct incorporation of cationic species larger than 2.61 Å, without using preintercalants, as is usually necessary when using the α-ZrP phase. We have successfully intercalated bioactive molecules such as cisplatin, doxorubicin, molybdocene dichloride, and insulin, among others.[35,38,42−45]

Insulin Delivery

Insulin is mainly administered intravenously to regulate glucose levels in diabetic patients. We reported the intercalation of insulin into ZrP nanoplatelets (Ins@ZrP) and suggested its use as an alternative oral delivery system.[45] X-ray powder diffraction (XRPD) data show an expanded interlayer distance of 29.3 Å for Ins@ZrP (Figure 2), consistent with insulin molecule's

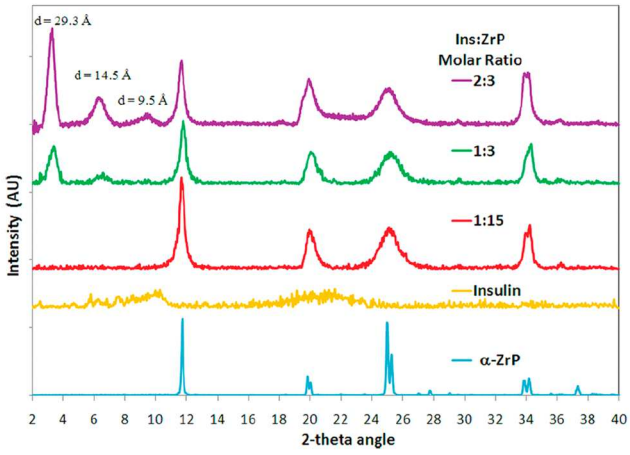

Figure 2. XRPD patterns of α-ZrP, insulin, and Ins@ZrP at different insulin:ZrP molar ratios. Reprinted with permission from reference 45. Copyright 2010 American Chemical Society.

dimensions and indicative of successful intercalation. If unintercalated θ-ZrP is dried, it converts to α-ZrP. Fourier Transformed Infrared Spectroscopy (FTIR) showed reduced relative intensity of the lattice water vibrational bands present in the ZrP spectrum (at 3590 cm^{-1}, 3510 cm^{-1}, and 3150 cm^{-1}) since insulin displaces water upon intercalation. The characteristic amide bands of insulin were observed at ca. 1500 cm^{-1} in the Ins@ZrP spectrum. In addition, a 28% loading of insulin into ZrP nanoplatelets was determined through thermogravimetric analysis (TGA).

Since Ins@ZrP was proposed for oral administration, drug release tests were performed in phosphate buffer solution at pH = 8.2 and 7.4. At pH = 8.2, ∼95% of insulin was released from ZrP nanoplatelets during the first 5 min, whereas at pH = 7.4 it took ∼30 min to release ∼90% of insulin. In the stomach's acidic environment, ZrP should protect insulin, preventing its denaturation, whereas at pH higher than 8.0, as in the intestine, ZrP is able to release insulin.[45]

Anticancer Drug Delivery

Cisplatin. In 2013, we reported the successful intercalation of cisplatin, an anticancer drug widely used as a treatment for different types of cancers,[46] into θ-ZrP nanoplatelets (CisPt@ZrP).[35] CisPt@ZrP intercalation was confirmed by XRPD (Figure 3), which showed an expanded interlayer distance of 9.3 Å. In addition, transmission electron microscopy (TEM, Figure 4) and X-ray elemental distribution "mappings" showed that ZrP partially retained its hexagonal shape with an average size of 180 nm, while Cl atoms in CisPt were exchanged by phosphate groups of the ZrP during the intercalation process; the platinum complexes are then covalently bonded to the layers.[35]

CisPt@ZrP's behavior under biological conditions was studied through drug release tests in simulated body fluid (SBF, pH = 7.4). Pt cumulative release percentage was between 2% and 3%, reaching a plateau after the first 12 h. When the drug release test was performed in artificial lysosomal fluid (ALF, pH = 4.5), the Pt cumulative release percentage from CisPt@ZrP was 50% after the first 12 h and 100% at 48 h. These findings demonstrate that CisPt@ZrP responds to a pH and chemical

https://doi.org/10.1021/accountsmr.1c00102
Acc. Mater. Res. 2021, 2, 793−803

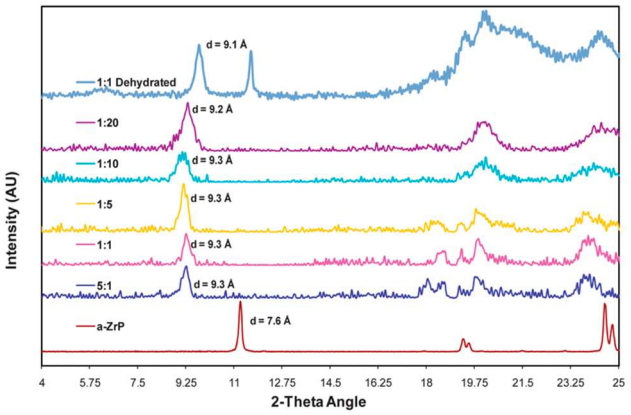

Figure 3. XRPD patterns of α-ZrP, and intercalation products at various CisPt:ZrP molar ratios (top to bottom: 1:20, 1:10, 1:5, 1:1, and 5:1). Reproduced from reference 35. Copyright 2013 Royal Society of Chemistry.

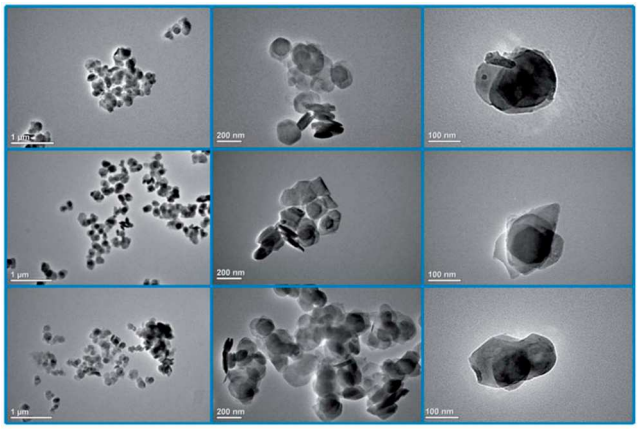

Figure 4. TEM images of CisPt@ZrP intercalation products at the (top row to bottom row) 1:5, 1:1, and 5:1 molar ratios. Reproduced from reference 35. Copyright 2013 Royal Society of Chemistry.

stimulus. In other words, ZrP can release the CisPt active species in the acidic environment of cancer cells' interior, while stabilizing the drug at pH = 7.4 and, by consequence, the cisplatin's toxicities due to its side effects related to non-selectivity would remain minimal.

Cell viability assays performed on a human breast adenocarcinoma cell line (MCF-7) demonstrated that CisPt@ZrP reduces 30% of the cell growth, but unintercalated ZrP nanoplatelets do not 1) affect the MCF-7 viability, 2) produce DNA damage, or 3) alter the MCF-7 cell cycle.

Molybdocene Dichloride. We successfully intercalated molybdocene dichloride (MDC), an organometallic anticancer drug with lower toxicity than cisplatin, into θ-ZrP nanoplatelets (MDC@ZrP).[44,47] Scanning Electron Microscopy/Energy Dispersive X-ray Spectroscopy (SEM-EDX) of MDC@ZrP showed no presence of Cl, which implies that the intercalated species could be the monocation $[Cp_2Mo(H_2O)(OH)]^+$.[44] This hypothesis is consistent with the XRPD results since the $[Cp_2Mo(H_2O)(OH)]^+$ dimensions are consistent with the expanded interlayer distance of 11.0 Å upon intercalation.

TEM images showed MDC@ZrP hexagonal shaped nanoplatelets with a size range of 75−200 nm. MDC@ZrP's FTIR spectrum showed the characteristic peaks of ZrP with a reduction in the intensity of the water vibrational bands compared to the unintercalated ZrP spectrum, due to displacement of water upon intercalation. Characteristic peaks of the Cp rings were observed at 3100 cm^{-1}, 1440 cm^{-1}, and 820 cm^{-1}. TGA showed that the amount of drug loaded into ZrP was 64%.

Doxorubicin. Doxorubicin (DOX) is one of the most widely used anticancer drugs.[48] DOX acts by intercalating its tetracycline ring into the DNA double helix; the stable DOX-DNA adduct sequesters the topoisomerase II genetic replication activity. In addition, the alteration of the p53 protein levels and other transcription factors as well as a free-radical related damage to DNA caused by DOX metabolites lead cells to apoptosis.[48] DOX is highly toxic to cancer and normal tissue as well. The lack of selectivity is responsible for DOX adverse effects, being kidney failure and cardiotoxicity the main cause of morbidity and mortality in patients.[48] New strategies are needed for selective delivery of DOX to cancerous tissue. Currently, most of the proposed DOX delivery systems are based on polymeric based encapsulation (e.g., DOXIL).

During the last 9 years we studied the intercalation, release, cytotoxicity, and biocompatibility of DOX incorporated into ZrP to develop a DOX nanocarrier system able to overcome the current limitations of free DOX therapy. In 2012, we reported the successful intercalation of DOX into ZrP;[44] the interlayer distance expanded to 20.3 Å in agreement with DOX dimensions if it arranges perpendicularly to the ZrP layers at full loading (34.9% according to TGA results). Interlayer distances of ca. 18 Å were obtained for the 25% and 14% loaded DOX@ZrP materials, suggesting a change in the DOX orientation inside the layers at those loading levels.[42]

Initially, we believed that the intercalation chemistry of DOX mainly involves an ion exchange mechanism where the protons of the phosphate groups from the interlayer space were exchanged and the remaining negatively charged oxygens were stabilized by electrostatic interactions with the positively charged amine group of DOX. Recent preliminary two-dimensional ^{31}P NMR experiments performed in collaboration with the University of Nantes in France raised new insights in the comprehension of the DOX intercalation process. Contrary to cisplatin intercalation, where the drug exchanges the phosphate protons and forms a Pt−O−P covalent bond, the 2-D ^{31}P NMR DOX@ZrP results reveal that deprotonation of phosphate groups does not take place. Moreover, DOX molecules intercalated in ZrP are stabilized by strong hydrogen bonding interactions. More specifically, the −OH from the hydroquinone and the amine group in the DOX molecule strongly interact with the protonated phosphate groups and the cointercalated water molecules inside the ZrP layers.

The DOX release mechanism from the ZrP interlayer space was also studied. Although a DOX release triggered by an acidic pH stimulus was proposed, a sustained diffusion mechanism was mostly observed. The DOX release was unsuccessful in PBS buffer at pH 5.4, 6.4, and 7.4. However, further release experiments in simulated body fluid (SBF) at pH 7.42 showed that for the 25% and 14% DOX@ZrP materials, 40% of the loaded DOX was released within the first 24 h and 80−88% within the next 11−14 days.[42] Those findings suggest that DOX releases by a diffusion mechanism which is coherent with the new ^{31}P NMR data mentioned above which shows that no proton exchange occurs upon intercalation. It is important to notice that cell viability assays showed IC_{50} values 50 and 2.7 times lower than free DOX when MCF-7 and MDA-MB 231 cell lines were exposed to DOX@ZrP after 48 and 96 h, respectively.[38,42] In addition, cellular uptake of DOX@ZrP

https://doi.org/10.1021/accountsmr.1c00102
Acc. Mater. Res. 2021, 2, 793−803

into MCF-7 and MDA-MB 231 cell lines was studied by confocal laser scanning microscopy (CLSM, Figure 5) using the

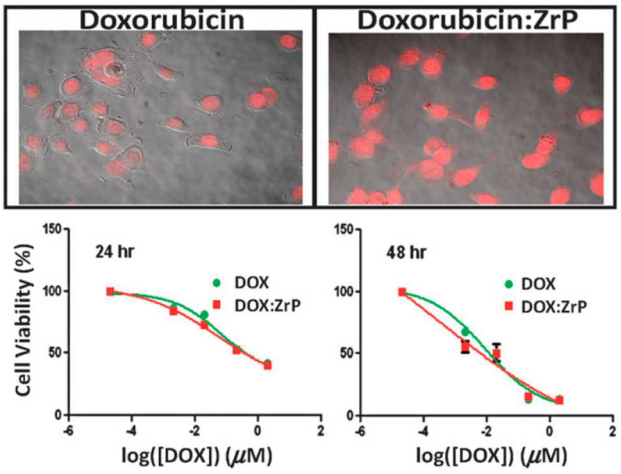

Figure 5. CLSM images and MTT results in breast cancer cells. Top: CLSM images of MCF-7 cells treated with DOX (left) and DOX:ZrP (right) showing higher uptake of DOX:ZrP nanoplatelets into the cells. Bottom: MTT assay resulting in MCF-7 cell lines at 24 and 48 h of exposure. Reproduced from reference 38. Copyright 2012 Royal Society of Chemistry. .

inherent fluorescent property of DOX. A higher cellular, including into the cell's nucleus, uptake of DOX after 4 h of exposure to DOX@ZrP nanoplatelets compared with free DOX was observed in both cell lines.[42] Therefore, two insights arose from these results: (i) a relative slow DOX release rate ensures that DOX@ZrP nanoplatelets reach their target, the tumor tissue, before releasing its cargo; (ii) the drug-release rate does not compromise the cytotoxic activity of intercalated DOX. We believe that a diffusion mechanism takes place intracellularly inducing DOX release from the ZrP nanoparticles. Biocompatibility studies reported no cytotoxicity related to nonintercalated ZrP nanoparticles.[42,43]

Five years ago, in collaboration with the Clearfield group, we started to develop multifunctional ZrP nanoparticles.[49,50] The high surface-charge density of one negative charge per 24 Å^2 provides a reactive surface able to be modified by organic and inorganic groups. In 2017, González-Villegas et al. reported the surface modification of DOX@ZrP.[50] The surface of DOX@ZrP was used as a platform to anchor poly(ethylene) glycol monophosphate (m-PEG-PO_3) molecules to improve the biocompatibility of the system, to reduce nanoparticles aggregation, and to eventually furtherly attach active targeting functionalities to the distal end of the m-PEG-PO_3 molecules. To do this, the DOX@ZrP surface was exchanged with Zr(IV) cations; negatively charged m-PEG-PO_3 molecules could then be attached to it. No changes in the interlayer distance (ca. 21 Å) of this DOX@ZrP material were observed in the XRPD diffractograms after the surface modification with Zr(IV) and m-PEG-PO_3 (m-PEG-PO_3/Zr(IV)/DOX@ZrP). This suggests that functionalization only occurred at the surface, as desired.

A comprehensive ^{31}P NMR analysis conducted by Bakhmutov et al. studied both Zr(IV) and m-PEG-PO_3 surfaces modified, but nonintercalated ZrP and DOX-intercalated ZrP materials.[49] The data allowed us to clearly assign a phosphorus reservoir for every phosphorus environment in the material: the peak at −21.4 ppm was assigned to the phosphate group interacting with the DOX molecules, the −27 ppm broad signal assigned to Zr(IV) exchanged surface phosphates in an approximately 20:1 HPO_4:PO_4^- molar ratio, and finally a weak resonance at −22.7 ppm confirmed the m-PEG-PO_3 anchoring on the Zr(IV) on the surface.

Preliminary release studies in SBF pH 7.42 solution showed that the DOX-release rate decreases for the fully surface functionalized nanoparticles, m-PEG−PO_3/Zr(IV)/DOX@ZrP. Interestingly, the m-PEG−PO_3/Zr(IV)/DOX@ZrP material reported almost 50% higher cytotoxic activity than free DOX within 48 h when human prostate cancer PC3 cells were exposed to it (Figure 6).[50] This result suggests that surface

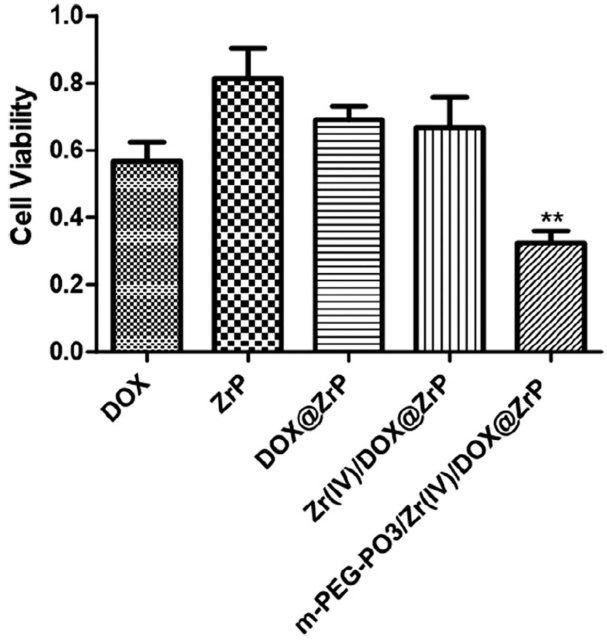

Figure 6. In vitro cytotoxicity of μM DOX, DOX@ZrP, Zr(IV)/DOX@ZrP, and m-PEG-PO_3/Zr(IV)DOX@ZrP to human prostate cancer PC3 cells after 48 h of incubation. Reprinted from *Inorganica Chimica Acta*, Vol. 468, González-Villegas, J.; Kan, Y.; Bakhmutov, V. I.; García-Vargas, A.; Martínez, M.; Clearfield, A.; Colón, J. L., Poly(ethylene glycol)-modified zirconium phosphate nanoplatelets for improved doxorubicin delivery, 270−279, Copyright 2017, with permission from Elsevier.

functionalization of DOX@ZrP nanoparticles with m-PEG-PO_3 increases the material stability under physiological simulated conditions while improving the cellular uptake resulting in stronger activity killing PC3 cancer cells.

■ ELECTROCATALYSIS

ZrP as Support Material for the Oxygen Evolution Reaction (OER) Active Species

One of the most pressing challenges of the 21st century is climate change.[51] Many scientists have embarked on tackling this challenge by developing new and innovative ideas on clean energy production and storage. From batteries to fuel cells, and other technologies, electrochemistry has played a central role in their development. Moreover, the half-cell reactions that need to be carried in many clean-energy production and storage apparatuses show kinetic sluggishness.

To reach broader implementation, many challenges need to be addressed, from governmental policies to scientific ones. For

https://doi.org/10.1021/accountsmr.1c00102
Acc. Mater. Res. 2021, 2, 793−803

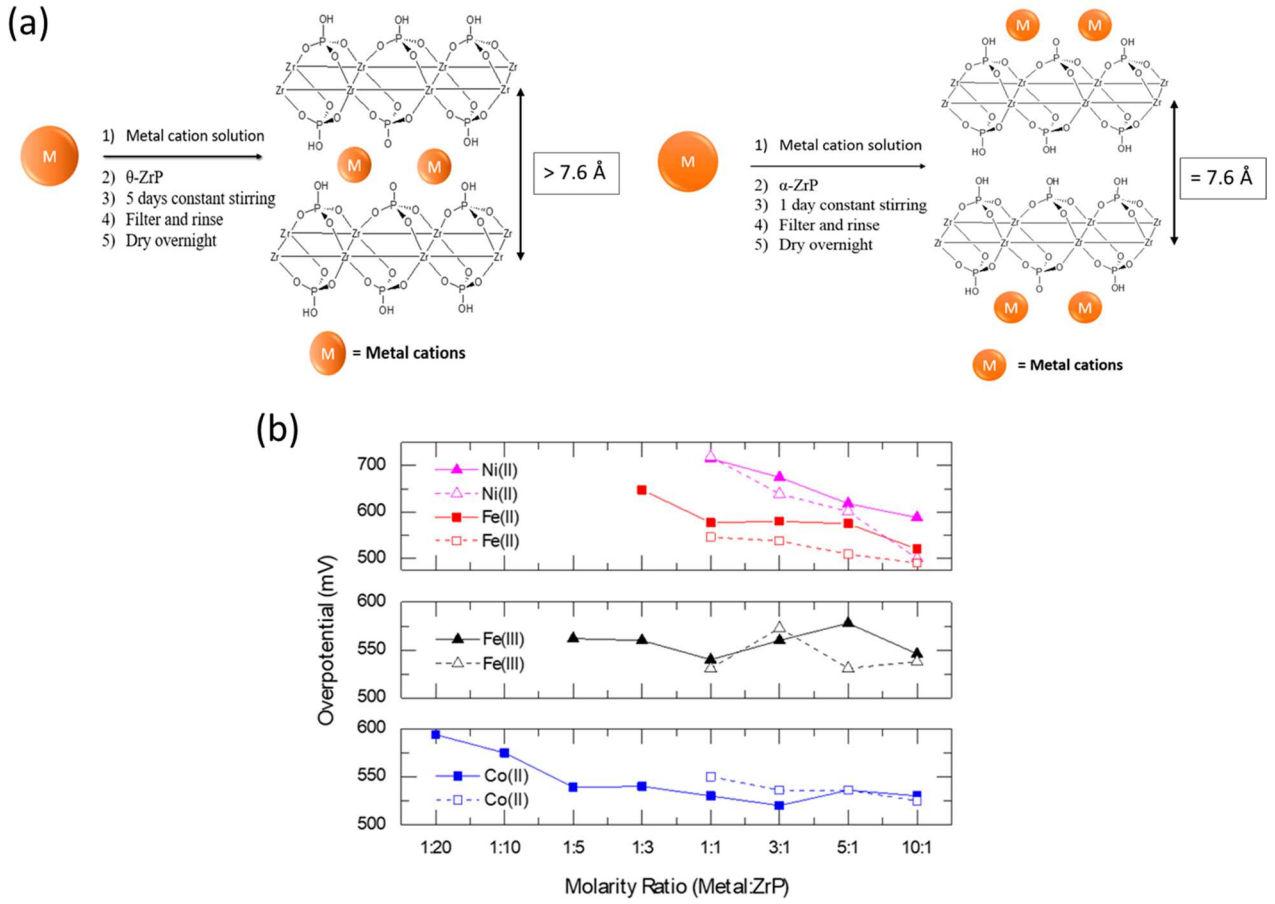

Figure 7. (a) Schematic representation of the synthesis procedure of intercalated (left) and surface adsorbed (right) ZrP catalysts. Reprinted from reference 58. (b) Overpotential as a function of M:ZrP ratio during synthesis. Dashed lines represent surface adsorbed catalysts and solid lines intercalated catalysts. Reprinted from reference 54.

example, the cost of a photoelectochemical (PEC) device for hydrogen production is dependent on many factors, including, but not limited to, the stability of the materials and their efficiency. The latter being a crucial challenge in technologies that run the OER as one of its half-cell reactions, such as, electrochemical CO_2 reduction, water electrolysis, metal-air batteries, and others. Due to the kinetic limitations stemming from the four proton−electron coupled oxidation steps of the OER (eqs 1−4 for alkaline media, where Cat stands for catalyst), high overpotential losses hinder the efficiency of such devices considerably.[52] Hence, the development of new and unconventional ideas for the study of OER catalysts are of much importance to this area of study.

$$\text{Cat} + \text{OH}^- \rightarrow \text{e}^- + \text{Cat-OH} \quad (1)$$

$$\text{Cat-OH} \rightarrow \text{e}^- + \text{H}^+ + \text{Cat-O} \quad (2)$$

$$\text{Cat-O} + \text{OH}^- \rightarrow \text{e}^- + \text{Cat-OOH} \quad (3)$$

$$\text{Cat-OOH} \rightarrow \text{e}^- + \text{Cat} + \text{H}^+ + \text{O}_2 \quad (4)$$

Advancements in OER catalysis have yielded important results that give insights into new strategies that can be implemented to improve energetic losses during the reaction. Two promising strategies are the use of confine environments in which the OER can take place and the use of supports that can provide synergistic electrochemical properties between the support and active species. Taking both points into consideration, we embarked into a new research application of ZrP: as support for active OER catalysts.[53]

ZrP properties make it a suitable material to be a support for host species for the OER. The OER is commonly performed under conditions that would compromise the integrity of many materials, such as very high or very low pH and high oxidative potentials (the thermodynamic potential of the reaction is 1.23 V vs the reversible hydrogen electrode (RHE)). The robustness of ZrP (e.g., high thermal and pH stability) and its electrochemical inertness propels it to be a promising candidate to be studied as an OER support. Not only that, but the presence of Brönsted acid (P−OH) groups at both the surfaces and the interlayer region allows it to ion-exchange OER species into and/or onto ZrP nanoparticles. This is particularly important as the OER could then be studied at the modified surfaces and at the interlayer region.

Intercalation of Metal Cations into ZrP

To study ZrP as a support platform for the OER, we first designed a composite material in which species that are known to show OER activity could be intercalated into ZrP. First-row transition metals are known to be OER active in alkaline conditions. Hence, the intercalation of different first-row transition metals, namely, Fe^{2+}, Fe^{3+}, Co^{2+}, and Ni^{2+}, was performed by using our method of direct intercalation using *θ*-ZrP.[58] However, Brönsted acid groups at the nanoparticle's surfaces would also ion-exchange during the intercalation procedure, thus producing a possible second active motif for

https://doi.org/10.1021/accountsmr.1c00102
Acc. Mater. Res. 2021, 2, 793−803

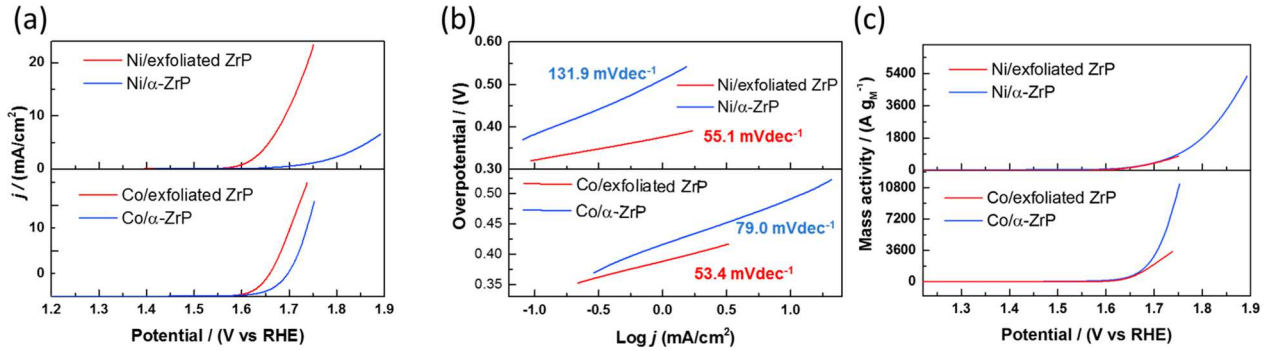

Figure 8. (a) Current density as a function of potential for the Ni-modified ZrP catalysts (top) and Co-modified ZrP catalysts (bottom). (b) Tafel plots for the Ni-modified ZrP catalysts (top) and Co-modified ZrP catalysts (bottom). (c) Mass normalized current as a function of potential for the Ni-modified ZrP catalysts (top) and Co-modified ZrP catalysts (bottom). Reproduced from reference 59. Copyright 2019 American Chemical Society.

catalysis to occur. To obtain a better understanding of this new intercalated catalyst, a second composite material was designed and synthesized in which the metal cations were only ion-exchanged onto the surfaces of ZrP. The use of α-ZrP works for this purpose as the metal cations (with their solvation shells) are too large to be intercalated into α-ZrP. The chemical physical characterization confirms that, indeed, both catalyst systems were successfully prepared. See Figure 7a for a schematic representation of both systems.

The catalysts were prepared by mixing a solution of the metal salt precursors with suspensions of either α-ZrP or θ-ZrP at different metal:ZrP synthesis molar ratios. Nonetheless, the atomic ratios in the products of these reactions were less than the synthesis molar ratios used, as determined by elemental composition analysis with X-ray photoelectron spectroscopy (XPS). It was found that as the synthesis molar ratio was increased during the reactions, so does the metal:Zr ratios (Figure S2), indicating a higher number of active sites. The intercalated catalysts contain far more metal species as expected due to the much higher surface area of these systems as not only the external surfaces are available for ion exchange but also the interlayer regions. Hence, these catalysts with higher loadings were expected to show higher activity for the OER in alkaline electrolyte (0.1 M KOH). The activity parameter used for comparing the activities of the different catalysts was the overpotential at a current density of 10 mA/cm^2 (η_{10}). Overpotential is typically defined as the additional potential to the thermodynamic equilibrium one needed to turn over the reaction. In this case, η_{10} would be the potential difference at the specified current density of 10 mA/cm^2. This parameter has been widely used to compare the catalytic activity of OER electrocatalysts in the literature, especially in the past decade.[55]

Several catalysts where synthesized with each metal in which the metal to ZrP molar ratio (M:ZrP) was systematically increased from 1:20 to 10:1. Figure 7b shows the results obtained for both catalyst systems. The *y*-axis represents the overpotential while the *x*-axis shows the different M:ZrP ratios used during the synthesis of catalysts. There are a few key takeaways from this data: (i) as the M:ZrP is increased during synthesis, the activity gradually improves and so does the loading as the M:Zr atomic ratios were observed to increase by XPS; (ii) surface adsorbed catalysts show equal or better activities than their intercalated counterparts synthesized at the same M:ZrP atomic ratios. The latter is an unexpected result as the catalyst system with the lower metal loading is the one that shows better OER performance. However, this leads to a new way of understanding the prepared metal-modified ZrP catalysts (in which each catalyst is modified only with one metal). Intercalated metals are possibly not electrochemically accessible to perform OER due to a variety of reasons, including mass transport limitations in which water is unable to access the active species in the interlayer, and or conductivity issues. Nonetheless, in a recent joint study with close collaborators, a mixed metal (NiFe) active motif inside the interlayer of ZrP was isolated.[56] A different joint study with other close collaborators also shows signs that if a molecular Co-porphyrin catalyst is intercalated into ZrP, activity coming from the interlayer can be observed.[57]

Meanwhile, our efforts were focused on improving the ZrP surface adsorbed catalysts. For this, we took advantage of ZrP chemistry. For decades, ZrP has been known to be able to be exfoliated into its nanosheets with the correct use of different intercalants. One of the most used strategies for ZrP exfoliation consists of the intercalation of small amines that have strong affinity to ZrP Brönsted acid groups.[53,58] When these amines are intercalated at a high enough concentration, cationic repulsions inside the layers will lead to exfoliation. Following this, an acid wash will displace the amines molecules and reproduce the (P−OH) groups. Ion exchange can then be performed on these nanosheets without the contamination of the exfoliating agents.

The ion exchange of Co^{2+} and Ni^{2+} cations onto ZrP nanosheets produces exfoliated materials with the advantage of having all metals on outside surfaces which are more easily accessible to the electrolyte and perform the OER.[59] These metal-modified systems were systematically studied against the previous Co^{2+} and Ni^{2+} surface-adsorbed catalysts.[54,59] In addition to overpotential, we further characterized the activities of these catalysts with their Tafel slopes. This is an electrokinetic parameter that helps in obtaining inherent kinetic information of the catalysts under study. In a Tafel analysis, the overpotential is plotted as a function of the logarithm of the current density. Hence, the slope of the line will inform the voltage necessary to increase the current density by a factor of 10.

Besides η_{10} and the Tafel analysis, mass activity was another parameter used to probe the activity of the catalysts. This parameter is of particular importance in the literature as it probes the intrinsic activity of the catalysts. It is also particularly important for industrial applications due to cost issues. When comparing η_{10} of the exfoliated catalysts to the surface adsorbed nanoparticles, a significant shift in the current to lower potentials is observed (Figure 8a). This shows that on a geometric basis, the exfoliated catalysts perform better. Additionally, the Tafel slopes (Figure 8b) of the exfoliated catalysts are lower, elucidating that for these catalysts, the higher loadings significantly affect the rate-limiting step. However, it is worth

https://doi.org/10.1021/accountsmr.1c00102
Acc. Mater. Res. 2021, 2, 793−803

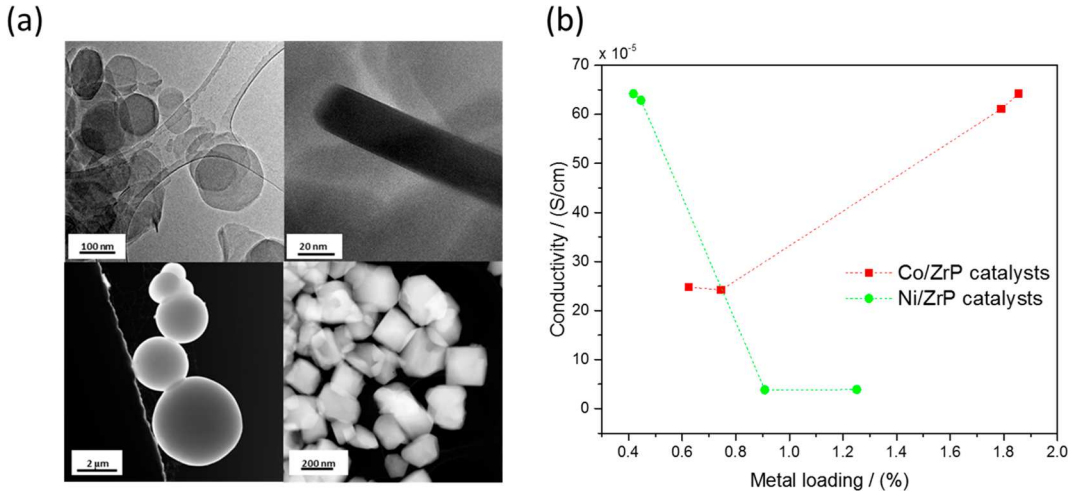

Figure 9. (a) TEM/STEM micrographs for the hexagonal (top-left), rods (top-right), spheres (bottom-left), and cube-like (bottom-right) ZrP supports. Reproduced with permission from ref 60. Copyright 2020 Royal Society of Chemistry. (b) Conductivity of the different Co and Ni ZrP catalysts with controlled morphology as a function of metal loading. Reproduced with permission from ref 60. Copyright 2020 Royal Society of Chemistry.

noting that the lower Tafel slopes can be due to several possible factors such as, improved kinetics, mass transport, and or electron transport. The mass activity analysis shows that the mass normalized current remains relatively equal except at higher potentials when the surface adsorbed catalysts show a higher normalized current (Figure 8c). This leads to the conclusion that the higher activity observed on a geometric basis was due to the much higher metal content that was observed through inductively couple plasma-mass spectrometry (ICP-MS) on the exfoliated catalysts and their higher accessibility to the electrolyte and not due to an intrinsic improvement on the activities of the metals on the ZrP support.

Morphology Control of ZrP

Several decades of ZrP research have led to the discovery of novel synthesis routes to produce ZrP with optimized properties for specific applications.[60] Interestingly, some of these produce ZrP particles with morphologies different from the common hexagonal platelets. A few of these morphologies were used to deposit Co^{2+} and Ni^{2+} via ion exchange for OER electrocatalysis. More specifically, ZrP mesoporous spheres, ZrP rods, ZrP cubes, and the common hexagonal platelets (Figure 9a) were used as hosts for the metal cations. Of these morphologies, the rods have the crystal structure of α-ZrP and the cubes are a previously reported phase known as τ'-ZrP (Figure S3).

The metal loading for these catalysts varies with the selection of the metal cation and the morphology used. The trend of increasing ion exchange for both metals was found to be in the order of spheres < cubes < rods < hexagonal platelets. However, Ni cations exchange in lower amounts when compared to Co cations. Besides loading, other factors such as electrical conductivity and the surface-area-to-volume ratio (SA:V) were examined. The latter was determined from the average measurements obtained through TEM/STEM micrographs. Both α-ZrP phases (hexagonal and rods) showed higher SA:V ratios than the cubes and spheres (least SA:V ratio). This shows that in the cobalt samples with the morphologies that have higher SA:V ratios, Co and Ni species obtain a higher coverage than the morphologies with lower SA:V ratios. As for electrical conductivity, the cobalt species show a trend of increasing conductivity with increasing loading. However, nickel species show an inverse trend as the conductivity decreases with increasing loading (Figure 9b).

The above-mentioned results explain the observed activities for the metal-modified ZrP catalysts on both a geometric and mass basis. The cobalt catalysts show an increase in activity when the loading is increased (geometric and mass activities). This shows that the higher coverage on Co species does not lead to conductivity losses. On the contrary, the activities for the nickel catalysts show that they decrease with increasing loading. This can be explained by their conductivity behavior and coverage on the ZrP particles. The increase in the loading and coverage of Ni leads to inactive areas due to the resistive species. Nonetheless, the ZrP spheres modified with Ni shows a remarkedly high mass activity. While the loading of this catalyst is the lowest, the high surface area of these spherical particles contributes to a low coverage of those resistive species and conductivity issues are possibly minimized, leading to its high mass activity. The mass activity of this catalyst of 272 A/g is slightly higher than commercial IrO_x (257 A/g) at an overpotential of 0.35 V. However, it is lower than state-of-the-art $NiFeO_xH_y$ catalyst (633 A/g), suggesting that mixed metals might help in improving the activities of ZrP catalysts for the OER. These mixed metal ZrP studies were developed by our collaborators. More specifically, intercalated mixed metal NiFe at different weight percentages (wt %) was systematically studied and compared against surface adsorbed NiFe catalysts. Impressively, an intercalated NiFe with a Fe composition of 90% shows a low η_{10} and high mass activity. This work highlights that the activity of this catalyst stems from the interlayer and isolates the active motif from surface or edge species.[56]

CONCLUSIONS

Our studies during the past 10−12 years have shown that ZrP is a versatile material with which to create new drug nanocarriers and efficient electrocatalytic OER systems. As we continue exploring new possibilities, we also need to focus on elucidating the particular geometrical arrangements that the drugs adopt inside the layers and the influence of ions and water in the intermolecular interactions and interactions with the layers. Further studies into how best to derivatize the surface of the nanoparticles to improve biocompatibility, circulation, and

https://doi.org/10.1021/accountsmr.1c00102
Acc. Mater. Res. 2021, 2, 793−803

selectivity will lead to optimization of systems for specific purposes. Envisioning future combined cancer nanotherapy applications, we are studying the intercalation chemistry and cytotoxic effects of layered systems having two drugs intercalated at the same time as well as a new stealth scheme. In addition, we are completing the design and development of schemes for active targeting of overexpressed receptors in cancer cells; studies on animal models are essential. In the electrocatalysis work, it is encouraging that a NiFe mixed metal OER catalytic system gives it best results at a Fe/(Fe+Ni) ratio of 90%, unique in this field, which suggest that the chemical microenvironment in ZrP could provide new efficient catalytic motifs based on earth-abundant catalysts.[56] Further studies, including operando measurements while obtaining XAS data in synchrotron facilities will allow us to gain insights into the nature of the active catalytic species. Mixed metal systems will be further studied, as well as bifunctional catalyst systems. We also look forward to studying intercalated earth-abundant metal catalysts in acidic media. By taking advantage of ZrP acid stability to provide a stable confined environment, we envision to stabilize these metals on a medium in which they have not been stable historically. The last 10 years of zirconium phosphate research has brought exciting new possibilities. More and more researchers are entering the field and are finding new applications for these materials such as ecofriendly nano flame retardants, toxic heavy metal removal for wastewater treatments, solar energy conversion, biomedicine, polymer nanocomposites, nuclear waste remediation, tribology, tissue repair, and anticorrosion additives, among many others.[1−3,5] The state of this field is very strong. Our dear old material has indeed a very bright future.

■ ASSOCIATED CONTENT

Supporting Information

The Supporting Information is available free of charge at https://pubs.acs.org/doi/10.1021/accountsmr.1c00102.

Schematic representation of the enhanced permeability and retention effect, atomic ratios, and structure of τ'-ZrP (PDF)

■ AUTHOR INFORMATION

Corresponding Author

Jorge L. Colón − *Department of Chemistry, University of Puerto Rico, San Juan, Puerto Rico 00925-2537, United States;* orcid.org/0000-0003-1398-2405; Email: jorge.colon10@upr.edu

Authors

Mario V. Ramos-Garcés − *Cain Department of Chemical Engineering, Louisiana State University, Baton Rouge, Louisiana 70803, United States;* orcid.org/0000-0002-7511-9941

Julissa González-Villegas − *Department of Chemistry, University of Puerto Rico, San Juan, Puerto Rico 00925-2537, United States*

Aleannette López-Cubero − *Department of Chemistry, University of Puerto Rico, San Juan, Puerto Rico 00925-2537, United States*

Complete contact information is available at: https://pubs.acs.org/10.1021/accountsmr.1c00102

Author Contributions

#M.V.R.-G., J.G-V, and A.L.-C. contributed equally. This manuscript was written through contributions of all authors. All authors have given approval to the final version of the manuscript.

Notes

The authors declare no competing financial interest.

Biographies

Mario V. Ramos-Garcés received his Ph.D. in Chemistry in 2020 from the Department of Chemistry, University of Puerto Rico, Río Piedras campus, under the supervision of Prof. Jorge L. Colón working on the electrocatalysis of the oxygen evolution reaction using nanostructured layered inorganic compounds. He then joined the group of Prof. Christopher G. Arges at Louisiana State University (now at Penn State University) as a postdoctoral researcher where his work focuses on the ionic activity and transport in nanostructured polymer electrolytes.

Julissa González-Villegas received her B.S. in Chemistry from the University of Puerto Rico, Río Piedras campus, in 2015 and is currently a Ph.D. candidate in Prof. Jorge L. Colón's group. Her research focuses on studying the intercalation and cointercalation of anticancer drugs using nanoparticles of zirconium phosphate for biomedical applications.

Aleannette López-Cubero received her B.S. in Education in Physics from the University of Puerto Rico, Río Piedras campus, in 2008 and is currently a Ph.D. candidate in Prof. Jorge L. Colón's group. Her research focuses on studying the intercalation of anticancer drugs using nanoparticles of zirconium phosphate covered with cancer cell membranes for biomedical applications.

Jorge L. Colón received his B.S. in Chemistry from the University of Puerto Rico, Río Piedras campus, in 1984 and a Ph.D. in Chemistry from Texas A&M University in 1989. He did postdoctoral research at Texas A&M University and was a National Science Foundation Postdoctoral Fellow at the California Institute of Technology. He then joined the Department of Chemistry at the University of Puerto Rico, Río Piedras in 1992, where he is currently professor and PI of the NSF-PREM Center for Interfacial Electrochemistry for Energy Materials (CIE^2M).

■ ACKNOWLEDGMENTS

This work was supported by the National Science Foundation under the NSF-PREM Center for Interfacial Electrochemistry of Energy Materials (CIE^2M) grant DMR-1827622, the NSF Center for Chemical Innovation in Solar Fuels CHE-1305124, and the Department of Energy SUNCAT Center for Interface Science and Catalysis DE-AC02-76SF00515. We acknowledge the Texas A&M University (TAMU) Microscopy and Imaging Center for the TEM facilities and the TAMU X-ray powder diffraction facilities. Río Piedras single crystal X-ray diffractometer at The University of Puerto Rico was acquired through the support of the NSF under the major instrumentation award CHE-1626103. M.V.R.-G. was supported by the NSF-PREM CIE^2 M grant, DMR-1827622. J.G.-V. acknowledges the Bridge to the Doctorate Fellowship from the Puerto Rico Louis Stokes Alliance for Minority Participation (PR-LSAMP) grant HRD-1826558, the UPR NASA Space Grant Program grant NNX15AI11H, and the Chateaubriand Fellowship of the France Embassy in Washington, D.C. A.L.-C. acknowledges the PEAF program of the University of Puerto Rico, Río Piedras. The authors acknowledge that part of this work was performed at the Stanford Nano Shared Facilities (SNSF), supported by the

National Science Foundation under award ECCS-1542152. Part of this work was performed at the Molecular Sciences Research Center and the Comprehensive Cancer Center of the University of Puerto Rico. The authors would also like to acknowledge the Materials Characterization Center of the University of Puerto Rico for the SEM micrographs and EDS spectra.

REFERENCES

(1) Xiao, H.; Liu, S. Zirconium phosphate (ZrP)-based functional materials: synthesis, properties and applications. *Mater. Des.* **2018**, *155*, 19−35.
(2) Cheng, Y.; Chuah, G. K. The synthesis and applications of α-zirconium phosphate. *Chin. Chem. Lett.* **2020**, *31*, 307−310.
(3) Bashir, A.; Ahad, S.; Malik, L. A.; Qureashi, A.; Manzoor, T.; Dar, G. N.; Pandith, A. H. Revisiting the old and golden inorganic material, zirconium phosphate: Synthesis, intercalation, surface functionalization, and metal ion uptake. *Ind. Eng. Chem. Res.* **2020**, *59*, 22353−22397.
(4) Colón, J. L.; Martí, A.; Sun, L. A life in crystallography. *Dalton Trans* **2020**, *49*, 3914−3916.
(5) Pica, M. Treatment of wastewaters with zirconium phosphate based materials: A review on efficient systems for the removal of heavy metal and dye water pollutants. *Molecules* **2021**, *26*, 2392.
(6) Clearfield, A.; Stynes, J. A.; J. The preparation of crystalline zirconium phosphate and some observations on its ion exchange behaviour. *J. Inorg. Nucl. Chem.* **1964**, *26*, 117−129.
(7) Clearfield, A.; Smith, G. D. The crystallography and structure of α-zirconium bis(monohydrogen orthophosphate) monohydrate. *Inorg. Chem.* **1969**, *8*, 431−436.
(8) Troup, J. M.; Clearfield, A. Mechanism of ion exchange in zirconium phosphates. 20. Refinement of the crystal structure of alpha-zirconium phosphate. *Inorg. Chem.* **1977**, *16*, 3311−3314.
(9) Alberti, G. Syntheses, crystalline structure, and ion-exchange properties of insoluble acid salts of tetravalent metals and their salt forms. *Acc. Chem. Res.* **1978**, *11*, 163−170.
(10) Clearfield, A. *Inorganic Ion Exchange Materials*; CRC Press: Boca Raton, 1982.
(11) Kumar, C. V.; Bhambhani, A.; Hnatiuk, N. Layered α-zirconium phosphates and phosphonates. In *Handbook of Layered Materials*; Scott, A., Carrado, K. A., Dutta, P. K., Eds.; Marcel Dekker: New York, 2004; pp 306−362.
(12) Laipan, M.; Xiang, L.; Yu, J.; Martin, B. R.; Zhu, R.; Zhu, J.; He, H.; Clearfield, A.; Sun, L. Layered intercalation compounds: Mechanisms, new methodologies, and advanced applications. *Prog. Mater. Sci.* **2020**, *109*, 100631.
(13) Alberti, G.; Torracca, E. Crystalline insoluble salts of polybasic metals − II. Synthesis of crystalline zirconium or titanium phosphate by direct precipitation. *J. Inorg. Nucl. Chem.* **1968**, *30*, 317−318.
(14) Alberti, G.; Costantino, U.; Allulli, S.; Tomassini, N. J. Crystalline $Zr(R\text{-}PO_3)_2$ and $Zr(R\text{-}OPO_3)_2$ compounds (R = organic radical). *J. Inorg. Nucl. Chem.* **1978**, *40*, 1113−1117.
(15) Clearfield, A.; Díaz, A. Zirconium phosphate nanoparticles and their extraordinary properties. In *Tailored Organic-Inorganic Materials*; Brunet, E., Colón, J. L., Clearfield, A., Eds.; Wiley: Hoboken, NJ, 2015; pp 1−44.
(16) Brunet, E.; De Victoria-Rodríguez, M.; Jiménez García-Patrón, L.; Hindawi, H.; Rodríguez-Payán, E.; Rodríguez-Ubis, J. C.; Juanes, O. Tales from the unexpected: Chemistry at the surface and interlayer space of layered organic-inorganic hybrid materials based on γ-zirconium phosphate. In *Tailored Organic-Inorganic Materials*; Brunet, E., Colón, J. L., Clearfield, A., Eds.; Wiley: Hoboken, NJ, 2015; pp 45−82.
(17) Kim, H.-N.; Keller, S. W.; Mallouk, T. Characterization of zirconium phosphate/polycation thin films grown by sequentiall adsorption reactions. *Chem. Mater.* **1997**, *9*, 1414−1421.
(18) Mosby, B. M.; Diaz, A.; Clearfield, A. Surface modification of layered zirconium phosphate: a novel pathway to multifunctional materials. *Dalton Trans* **2014**, *43*, 10328.
(19) Casciola, M. From layered zirconium phosphates and phosphonates to nanofillers for ionomeric membranes. *Solid State Ionics* **2019**, *336*, 1−10.
(20) Brunet, E.; Alonso, M.; Cerro, C.; Juanes, O.; Rodriguez-Ubis, J. C.; Kaifer, A. E. A luminescence and electrochemical study of photoinduced electron transfer within the layeres of zirconium phosphate. *Adv. Funct. Mater.* **2007**, *17*, 1603−1610.
(21) Martí, A. A.; Colón, J. L. Photophysical characterization of tris(2,2-bipyridyl)ruthenium(II) ion-exchanged within zirconium phosphate. *Inorg. Chem.* **2010**, *49*, 7298−7303.
(22) Santiago-Berríos, M. B.; Declet-Flores, C.; David, A.; Borrero, S.; Vélez, M. M.; Díaz-Díaz, A.; Guadalupe, A. R.; Colón, J. L. Direct intercalation of bis-2,2',2",6-terpyridyl cobalt (III) into zirconium phosphate layers for biosensing applications. *Langmuir* **2012**, *28*, 4447−4452.
(23) Santiago, M. B.; Declet-Flores, C.; Díaz, A.; Vélez, M. M.; Bosques, M. Z.; Sanakis, Y.; Colón, J. L. Layered inorganic materials as redox agents: ferrocene-intercalated zirconium phosphate. *Langmuir* **2007**, *23*, 7810−7817.
(24) Rivera, E. J.; Barbosa, C.; Torres, R.; Rivera, H.; Fachini, E. R.; Green, T. W.; Connick, W. B.; Colón, J. L. Luminescence rigidochromism and redox chemistry of pyrazolate-bridged binuclear platinum(II) diimine complex intercalated into zirconium phosphate layers. *Inorg. Chem.* **2012**, *51*, 2777−2784.
(25) Puglia, M. K.; Malhotra, M.; Kumar, C. V. Engineering functional inorganic nanobiomaterials: controlling interactions between 2D-nanosheets and enzymes. *Dalton Trans* **2020**, *49*, 3917−3933.
(26) He, X.; Xiao, H.; Choi, H.; Díaz, A.; Mosby, B.; Clearfield, A.; Liang, H. α-Zirconium phosphate nanoplatelets as lubricant additives. *Colloids Surf., A* **2014**, *452*, 32−38.
(27) Kijima, T. Direct preparation of θ-zirconium phosphate. *Bull. Chem. Soc. Jpn.* **1982**, *55*, 3031−3032.
(28) Martí, A. A.; Rivera, N.; Soto, K.; Maldonado, I.; Colón, J. L. Intercalation of $Re(phen)(CO)_3Cl$ in a zirconium phosphate framework: a water insoluble inorganic complex immobilized in a highly polar lamellar matrix. *Dalton Trans* **2007**, 1713−1718.
(29) Cho, K.; Wang, X.; Nie, S.; Chen, Z.; Shin, D. M. Therapeutic nanoparticles for drug Delivery in cancer. *Clin. Cancer Res.* **2008**, *14*, 1310−1316.
(30) Maeda, H. The enhanced permeability and retention (EPR) effect in tumor vasculature: The key role of tumor-selective macromolecular drug targeting. *Adv. Enzyme Regul.* **2001**, *41*, 189−207.
(31) Li, R.; Liu, T.; Wang, K. Hyaluronic acid-modified zirconium phosphate nanoparticles for potential lung cancer therapy. *Biomed. Tech.* **2017**, *62*, 67−73.
(32) Pattni, B. S.; Chupin, V. V.; Torchilin, V. P. New developments in liposomal drug delivery. *Chem. Rev.* **2015**, *115*, 10938−10966.
(33) Cabral, H.; Miyata, K.; Osada, K.; Kataoka, K. Block copolymer micelles in nanomedicine applications. *Chem. Rev.* **2018**, *118*, 6844−6892.
(34) Zhai, J.; Luwor, R. B.; Ahmed, N.; Escalona, R.; Tan, F. H.; Fong, C.; Ratcliffe, J.; Scoble, J. A.; Drummond, C. J.; Tran, N. Paclitaxel-loaded self-assembled lipid nanoparticles as targeted drug delivery systems for the treatment of aggressive ovarian cancer. *ACS Appl. Mater. Interfaces* **2018**, *10*, 25174−25185.
(35) Díaz, A.; González, M. L.; Pérez, R. J.; David, A.; Mukherjee, A.; Báez, A.; Clearfield, A.; Colón, J. L. Direct intercalation of cisplatin into zirconium phosphate nanoplatelets for potential cancer nanotherapy. *Nanoscale* **2013**, *5*, 11456−11463.
(36) Wang, Y.; Pi, C.; Feng, X.; Hou, Y.; Zhao, L.; Wei, Y. The influence of nanoparticle properties on oral bioavailability of drugs. *Int. J. Nanomed.* **2020**, *15*, 6295−6310.
(37) Clearfield, A.; Ortiz-Avila, C. Y. Polyether and polyimine derivatives of layered zirconium phosphates as supramolecules. In *Supramolecular Architecture: Synthetic Control in Thin Films and Solids*; Bein, T., Ed.; ACS Symposium Series 499; American Chemical Society: Washington, DC, 1992; pp 178−193.
(38) Díaz, A.; Saxena, V.; González, J.; David, A.; Casañas, B.; Carpenter, C.; Batteas, J. D.; Colón, J. L.; Clearfield, A.; Hussain, M. D.

Zirconium phosphate nano-platelets: A novel platform for drug delivery in cancer therapy. *Chem. Commun.* **2012**, *48*, 1754−1756.
(39) Liu, Y.; Tan, J.; Thomas, A.; Ou-Yang, D.; Muzykantov, V. R. The shape of things to come: Importance of design in nanotechnology for drug delivery. *Ther. Delivery* **2012**, *3*, 181−194.
(40) Truong, N. P.; Whittaker, M. R.; Mak, C. W.; Davis, T. P. The importance of nanoparticle shape in cancer drug delivery. *Expert Opin. Drug Delivery* **2015**, *12*, 129−142.
(41) Prabhakar, U.; Maeda, H.; Jain, R. K.; Sevick-Muraca, E. M.; Zamboni, W.; Farokhzad, O. C.; Barry, S. T.; Gabizon, A.; Grodzinski, P.; Blakey, D. C. Challenges and key considerations of the enhanced permeability and retention effect for nanomedicine drug delivery in oncology. *Cancer Res.* **2013**, *73*, 2412−2417.
(42) Saxena, V.; Diaz, A.; Clearfield, A.; Batteas, J. D.; Hussain, M. D. Zirconium phosphate nanoplatelets: A biocompatible nanomaterial for drug delivery to cancer. *Nanoscale* **2013**, *5*, 2328−2336.
(43) González, M. L.; Ortiz, M.; Hernández, C.; Cabán, J.; Rodríguez, A.; Colón, J. L.; Báez, A. Zirconium Phosphate Nanoplatelet Potential for Anticancer Drug Delivery Applications. *J. Nanosci. Nanotechnol.* **2016**, *16*, 117−129.
(44) Casañas-Montes, B.; Díaz, A.; Barbosa, C.; Ramos, C.; Collazo, C.; Meléndez, E.; Queffelec, C.; Fayon, F.; Clearfield, A.; Bujoli, B.; Colón, J. L. Molybdocene dichloride intercalation into zirconium phosphate nanoparticles. *J. Organomet. Chem.* **2015**, *791*, 34−40.
(45) Díaz, A.; David, A.; Pérez, R.; González, M. L.; Báez, A.; Wark, S. E.; Zhang, P.; Clearfield, A.; Colón, J. L. Nanoencapsulation of insulin into zirconium phosphate for oral delivery applications. *Biomacromolecules* **2010**, *11*, 2465−2470.
(46) Martinho, N.; Santos, T. C. B.; Florindo, H. F.; Silva, L. C. Cisplatin-membrane interactions and their influence on platinum complexes activity and toxicity. *Front. Physiol.* **2019**, *9*, 1898.
(47) Kandioller, W.; Reikersdorfer, M.; Theiner, S.; Roller, A.; Hejl, M.; Jakupec, M. A.; Malarek, M. S.; Keppler, B. K. The impact of leaving group variation on the anticancer activity of molybdenocenes. *Organometallics* **2018**, *37*, 3909−3916.
(48) Mitry, M. A.; Edwards, J. G. Doxorubicin induced heart failure: Phenotype and molecular mechanisms. *Int. J. Cardiol. Heart Vasc.* **2016**, *10*, 17−24.
(49) Bakhmutov, V. I.; Kan, Y.; Sheikh, J. A.; González-Villegas, J.; Colón, J. L.; Clearfield, A. Modification and intercalation of layered zirconium phosphates: A solid-state NMR monitoring. *Magn. Reson. Chem.* **2017**, *55*, 648−654.
(50) González-Villegas, J.; Kan, Y.; Bakhmutov, V. I.; García-Vargas, A.; Martínez, M.; Clearfield, A.; Colón, J. L. Poly(ethylene glycol)-modified zirconium phosphate nanoplatelets for improved doxorubicin delivery. *Inorg. Chim. Acta* **2017**, *468*, 270−279.
(51) IPCC. *Climate Change 2021: The Physical Science Basis*. Contribution of Working Group I to the Sixth Assessment Report of the Intergovernmental Panel on Climate Change; Masson-Delmotte, V. et al., Eds.; Cambridge University Press. In Press
(52) Seh, Z. W.; Kibsgaard, J.; Dickens, C. F.; Chorkendorff, I.; Nørskov, J. K.; Jaramillo, T. F. Combining Theory and Experiment in Electrocatalysis: Insights into Materials Design. *Science* **2017**, *355*, No. eaad4998.
(53) Ramos-Garcés, M. V.; Sanchez, J.; Barraza Alvarez, I.; Wu, Y.; Villagrán, D.; F. Jaramillo, T.; L. Colón, J. Water splitting electrocatalysis within layered inorganic nanomaterials. In *Water Chemistry*; Eyvaz, M., Yüksel, E., Eds.; IntechOpen: London, 2020; pp 201−217.
(54) Sanchez, J.; Ramos-Garcés, M. V.; Narkeviciute, I.; Colón, J. L.; Jaramillo, T. F. Transition metal-modified zirconium phosphate electrocatalysts for the oxygen evolution reaction. *Catalysts* **2017**, *7*, 132.
(55) McCrory, C. C. L.; Jung, S.; Ferrer, I. M.; Chatman, S. M.; Peters, J. C.; Jaramillo, T. F. Benchmarking hydrogen evolving reaction and oxygen evolving reaction electrocatalysts for solar water splitting devices. *J. Am. Chem. Soc.* **2015**, *137*, 4347−4357.
(56) Sanchez, J.; Burke Stevens, M.; Young, A. R.; Gallo, A. A.; Zhao, M.; Liu, Y.; Ramos-Garcés, M. V.; Ben-Naim, M.; Colón, J. L.; Sinclair, R.; King, L. K.; Bajdich, M.; Jaramillo, T. F. Isolating the electrocatalytic activity of a confined NiFe motif within zirconium phosphate. *Adv. Energy Mater.* **2021**, *11*, 2003545.
(57) Barraza Alvarez, I.; Wu, Y.; Sanchez, J.; Ge, Y.; Ramos-Garcés, M. V.; Chu, T.; Jaramillo, T. F.; Colón, J. L.; Villagrán, D. Cobalt porphyrin intercalation into zirconium phosphate layers for electrochemical water oxidation. *Sustain. Energy Fuels* **2021**, *5*, 430−437.
(58) Ramos-Garcés, M. V.; Colón, J. L. Preparation of zirconium phosphate nanomaterials and their applications as inorganic supports for the oxygen evolution reaction. *Nanomaterials* **2020**, *10*, 822.
(59) Ramos-Garcés, M. V.; Sanchez, J.; Del Toro-Pedrosa, D. E.; Barraza Alvarez, I.; Wu, Y.; Valle, E.; Villagrán, D.; Jaramillo, T. F.; Colón, J. L. Transition metal-modified exfoliated zirconium phosphate as an electrocatalyst for the oxygen evolution reaction. *ACS Appl. Energy Mater.* **2019**, *2*, 3561−3567.
(60) Ramos-Garcés, M. V.; Sanchez, J.; La Luz-Rivera, K.; Del Toro-Pedrosa, D. E.; Jaramillo, T. F.; Colón, J. L. Morphology control of metal-modified zirconium phosphate support structures for the oxygen evolution reaction. *Dalton Trans* **2020**, *49*, 3892−3900.

https://doi.org/10.1021/accountsmr.1c00102
Acc. Mater. Res. 2021, 2, 793−803